Feng Ye [1,2]
Zihan Zhao[2]
Songqi Gui[3*]
Zhenyu Gao[3]

Construction of Spatial Experience and Interaction Model of Industrial Heritage Based on Virtual Reality Technology

Journal of Electrical Systems

Abstract: **-** The term "industrial heritage" describes the tangible remnants of a society's industrialization and economic growth, including buildings, locations, and artefacts. Various features such as factories, mills, mines, railroads, industrial machinery, warehouses, and other industrial infrastructure are all part of this history. These material remains serve as a testament to the changes that industrialization brought about in terms of technology, society, and the economy. In this manuscript, Construction of Spatial Experience and Interaction Model of Industrial Heritage Based on Virtual Reality Technology (BVR-SE-IMIH-TINN) are proposed. Initially input data is gathered from real time data is taken from camera or mobile phone. To execute this, input image is pre-processed using Generalized Multi-kernel Maximum Correntropy Kalman Filter (GMMCKF), it removes the noise from collected the data; then the Pre-processed data is feature extracted using Synchro spline-kernelled chirplet extracting transform (SSCET). In feature extraction SSCET is extract some feature such as Geometric features likes area, slope, centroids and perimeter. Then, the extracted data is fed to Thermodynamics-Informed Neural Network (TINN) for effectively categorize Interaction Model of Industrial Heritage. In general, TINN doesn't express adapting optimization approaches to determine optimal parameters to ensure accurate virtual reality heritage picture collection. Hence, the Binary Arithmetic Optimization Algorithm (BAOA) to optimize Heterogeneous Thermodynamics-Informed Neural Network which accurately categorized the industrial heritage. Then the proposed BVR-SE-IMIH-TINN is implemented and the performance metrics such as Accuracy, Recall, Precision, F1- Score, Specificity, and Computation Time are analyzed. Performance of BVR-SE-IMIH-TINN approach attains 18.41%, 24.08% and 32.57% higher accuracy, 19.21%, 20.08% and 21.57% higher recall and attains 20.31%, 21.08% and 22.57% higher precision when analyzed with existing techniques likes intelligent splicing method of virtual reality Lingnan cultural heritage panorama depend on automatic machine learning (ISM-VLHP-AML), key technologies of digital protection of historical with cultural heritage depend on virtual reality technology (DPH-CH-VRT), Reconstruction of Industrial and Historical Heritage for Cultural Enrichment Utilizing Virtual and Augmented Reality (RI-HCE-VAR) methods respectively.

Keywords: Binary Arithmetic Optimization Algorithm, Generalized Multi-kernel Maximum Correntropy Kalman Filter, Industrial Heritage, Multimedia Knowledge Graph and Deep Learning Techniques, Synchro spline-kernelled chirplet extracting transform, Thermodynamics-Informed Neural Network.

I. INTRODUCTION

The quality and efficiency of picture registration, which is the first stage of image splicing, are crucial in deciding the outcome [1]. Despite being reasonably mature and widely used, the generally utilized image registration techniques represents SIFT algorithm still require additional optimization and improvement due to the algorithm's huge computation requirements, somewhat long operating times, and very general accuracy. Lingnan culture encompasses a wide range of topics, including academic study, literature, art, calligraphy, music, gardens, folklore, religion, opera, crafts, architecture, cuisine, language, overseas Chinese culture [2]. It is specifically associated with the Lingnan region of China [3]. Regarding picture stitching technology, it's a full process that involves image gathering and stitching [4]. However, most academic research done now focuses on a single data point in the process, leaving no standardized, effective answer [5]. Therefore, this study has to investigate and provide a plausible answer on its own when working on investigate of Lingnan cultural heritage panorama show technology depend on image mosaic [6, 7]. As panoramic stitching technology develops, image-depend virtual reality technology becomes more engaging. Advanced computer-generated technology called virtual reality immersion (VRI) lowers subjective ratings of discomfort during procedural medical treatments [8]. According to VRI lowers pain-related brain activity as determined by functional magnetic resonance imaging [9]. Utilizing special goggles otherwise computer, they assigned 24 patients by chronic itching—16 with dermatitis-induced psoriasis vulgaris, 8 with psoriasis vulgaris—randomly to interactive computer game screen [10]. Use a visual analogy scale (range from 0 to 10) to self-assess the level of itching before, during, and 10 minutes after exposure. Despite the fact that their research procedures only included twenty-four persistent pruritus individuals, the study's sample size was insufficient [11]. According to Bastug et

[1]School of Design and Art, Communication University of Zhejiang, Hangzhou, Zhejiang 314500, China
[2]School of Design, Central Academy of Fine Arts, Beijing 100102, China
[3] Nanchang Vocational Institute of Film and Television Communication, Nanchang, Jiangxi 330000, China,
Feng Ye: yefeng@cuz.edu.cn
Zihan Zhao: zhaozihan931117@163.com

al., success of immersive VR experiences hinges resolving a variety of problems across several academic fields. For their research, they made use of artificial intelligence, computer vision, fog/edge computing, storage/memory, and more [12].

After a description of the fundamental criteria for a wireless connection, certain important components are introduced. Furthermore, while studying three VR case studies, producing numerical outcomes under varied network, storage, calculation configurations, investigate methodology defies logic. Environmental factors and mental health disorders are inextricably linked. Freeman et al. believe that, by VR and computer-generated interactive environments, individuals regularly experience their problematic situations, learn how to overcome problems during evidence-depend psychotherapy. They carried out an organized analysis of empirical studies. A total of 285 studies were found, 86 of which included treatments, 45 theoretical advancements, and evaluations [13]. Anxiety, schizophrenia, drug-related illnesses, and eating disorders are the primary ailments under investigation [14]. Despite the fact that his research has identified numerous therapy approaches, their research methodology is irrational [15]. The intelligent mosaic approach of the VR Lingnan cultural heritage panorama, which is depends on AML is the major topic of this research. To mitigate the impact of not enough camera regulation, gather images based on overlap area among nearby images of suitable size, it is imperative to minimize the negative effects of the collection process on final panoramic image of Lingnan cultural heritage [16]. Image demonising and image projection modification are the two main image pre-processing techniques used to improve the visual effects of Lingnan cultural heritage panoramic photos [17].The optimum suture line position should take into account the least amount of colour difference in suture area, most same texture on both sides [18]. It is depend on number of pixels in first row of overlapping area to identify candidate suture line column [19].

A. Problem statement and Motivation behind this Research work

The conditions needed for a wireless connection after describing VR, a few important components are introduced. Furthermore, their research methodology defies logic, despite the fact that have examined three VR case studies, produced numerical data under diverse storage, computation, network configurations. Environmental factors and mental health disorders are inextricably linked. Through computer-generated interactive environments and virtual reality (VR), people can relive their troublesome situations; learn how to overawe them with evidence-depend psychotherapy [20-25].

This paper specifies the shooting scenario selection criteria throughout the research and testing process. It is used to reduce the camera's irregularly rotating motion and gather photos based on the amount of overlap between neighbouring, suitably sized images and these functions as the initial stage that precedes image fusion and registration.

B. Contribution.

The major contribution of this paper includes,

- The proposed approach is presenting Thermodynamics-Informed Neural Networks for Virtual Reality-Based Spatial Experience and Interaction Model of Industrial Heritage.
- The field of Spatial Experience and Interaction Model of Industrial Heritage is used to GMMCKF and the Synchro spline-kernelled chirplet extraction transform.
- A creative, comprehensive strategy and theoretical framework that uses virtual reality (VR) technologies to digitally depict the long-term changes in a heritage site while testing the validity and dependability of the framework.

Remaining manuscript is arranged as below: part 2 presents literature review, part 3 describes proposed method, part 4 proves result with discussion, part 5 concludes the manuscript.

II. LITERATURE REVIEW

Several investigate works were previously suggested based on Interaction Model of Industrial Heritage. A few works are reviewed here,

Fu et al. [20] have presented ISM of virtual reality Lingnan cultural heritage panorama depend on AML. In this study panorama of Lingan cultural heritage is constructed by using cylindrical projection. They first do image segmentation for all Lingnan cultural heritage training image in order to obtain several areas, extract visual attributes of all area. They utilize AML methods to train visual feature set, apply bagging technique to create various training subset. To select the optimal stitching line during the stitching implementation, they first

evaluate overlap region of two images based on matched SIFT feature points to heterogeneities all component classifier. This method provides higher accuracy but it provides lower f1 score.

Zhang [21] has presented Key Technologies of DPH with Cultural Heritage depend on VRT. The images' feature points were extracted using Harris operator, two registered images were computed based on affine transformation coefficient. In order to achieve seamless mosaic design of images and forward, backward projection process of circular panoramic images, images experience affine transformation and were then bilinear interpolated, weighted smoothed based on nearby location of overlapping area. Also research creative expression of acquiring 3D panoramic images. This method provides higher accuracy but it provides lower recall.

Paulauskas et al. [22] have presented Reconstruction of Industrial and Historical Heritage for Cultural Enrichment Utilizing VAR. Designs, builds, test VR for kinaesthetic distant learning in museum setting. A virtual reality training tool created that allows students to choose and act out pre-made scenarios in a virtual setting. Kinaesthetic learning features underpin the program's interaction. For learners, VR-controlled scenarios imitate real-world physical engagement with items. The purpose was to evaluate VR educational program's efficacy in comparison to other forms of instructional materials. They have developed a solution that integrates their 3D images with rendering capabilities. This method provides higher precision but it provides lower accuracy.

Deng et al. [23] have presented research on CNN-depend VR platform framework for intangible cultural heritage conservation of China Hainan Li nationality: boat-shaped house as example. Here, enumerates and analyses different incidents, academic directions of intangible cultural heritage, combined by existing status of intangible cultural heritage in Hainan. These all present stricter guidelines for preserving Hainan's cultural legacy, emphasizing the need to do so by using not only conventional methods but also the benefits of modern scientific and technology advancements to stay relevant. This method provides higher specificity but it provides lower recall.

Khan et al. [24] has presented Using augmented reality and deep learning to improve Taxila Museum experience. An attempt was made to enrich user’s museum experience by important multimedia information with for developing better connection with artefacts with the Taxila Museum in Pakistan that has magnificently maintained Gandhara civilization. The suggested remedy is Augmented Reality smart phone application that utilizes DL to identify artefacts in real time, provides visitors with helpful multimedia content Utilizing pertinent assessment models such as the triptych model of interaction and the Museum Experience Scale (MES), the evaluation is meticulously carried out. This method provides higher recall but it provides lower accuracy.

Rinaldi et al. [25] have presented Augmented Reality CBIR System Depend on Multimedia Knowledge Graph and DL Methods in Cultural Heritage. This paper offers a mobile augmented reality system that uses linked open data and content-based picture analysis algorithms to increase user understanding of cultural assets. Specifically, they investigate the applications of conventional feature extraction approaches as well as a novel approach that makes use of deep learning methods. In addition, they perform an exhaustive experimental analysis to identify the optimal technique for accurately extracting multimedia elements for cultural heritage analysis. This method provides specificity but it provides lower f1- score.

III. PROPOSED METHODOLOGY

In this proposed methodology, Construction of Spatial Experience and Interaction Model of Industrial Heritage Based on Virtual Reality Technology (BVR-SE-IMIH-TINN) are discussed for identifying Virtual Reality-Based Spatial Experience and Interaction Model of Industrial Heritage. The model endures initial image gathering by accurately identifying the presence, location, and characteristics further processing. These phases endure major three processes likes preprocessing, feature extraction, and Heritage Picture Collectionin succeeding sectors. Block diagram of BVR-SE-IMIH-TINN is represented by Figure 1.

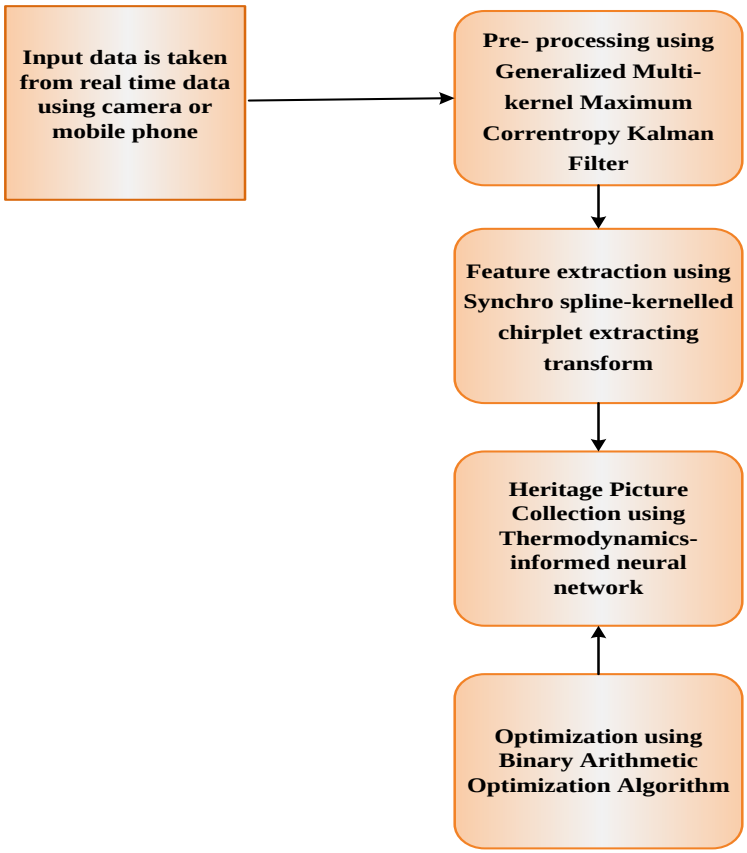

Figure1: Block Diagram for Proposed BVR-SE-IMIH-TINN Method

A. Data acquisition

The input data are taken from real time dataset [20] using camera or mobile phone. It collected from4 several kinds of data projection transformations, specifically planar projection, cube projection, spherical projection, cylindrical projection. It is varied projections will have very varied building techniques and visual quality. Input data are then fed to feature extraction process respectively.

B. Pre-processing using Generalized Multi-kernel Maximum Correntropy Kalman Filter

In this section, GMMCKT [26] technique is utilized which used to remove the noise from the collected input image. This proposal suggests using multiple kernels to extend the notion of maximum Correntropy. Functions called kernels convert input data into a higher-dimensional space so that non-linear correlations can be recorded. Several kernels are combined in generalized multi-kernel techniques to improve the model's capacity to identify intricate patterns in the image. Among them, the disturbance observer based on the Kalman filter is appealing as it estimates disturbance, state simultaneously and works best for linear system and Gaussian noises. Initially, Correntropy was described as a measure of local resemblance between two random variables. Thus it is given in equation (1)

$$C(X,Y) = E[k(X,Y)] \tag{1}$$

Here, X,Y is defined as random variable; E is denotes the energy level; k is denotes the kind of distribution and C is denotes join distribution. A common used kernel is Gaussian density function. Thus it is given in equation in (2)

$$k(x,y) = G_{\alpha,\beta}(x,y) = \exp(-|e/\beta|^{\alpha}) \tag{2}$$

Here, $k(x,y)$ represents shift- invariant Mercer kernel; $x\,and\,y$ represents realization of $X\,and\,Y$; α is represented the shape parameter; β is represented by the kernel bandwidth; G is represented the Gaussian density function and e is represented the true function of $x-y$. Then the join distribution of random variable is defined by the initialize the random variable. Thus it is given in equation (3)

$$C(X,Y)=\sum_{i=1}^{l}\beta_i^{\alpha}C_{\alpha,\beta_i}(X_i,Y_i) \tag{3}$$

Where, Here, X,Y is defined as random variable; C is denotes join distribution; X_i,Y_i is defined as the initialization of random variable; α is represents shape parameter, β represents kernel bandwidth. Then join distribution is not available and only samples N can be obtained. Thus it is given in equation (4)

$$C_{\alpha,\beta_i}(X_i,Y_i)=\frac{1}{N}\sum G_{\alpha,\beta_i}(x_i(k),y_i(k)) \tag{4}$$

Here, X,Y is defined as random variable; k is denotes the kind of distribution and C is denotes join distribution; G is represented the Gaussian density function; α is represented the shape parameter; β is represented by the kernel bandwidth; N is denotes the only sample function and X_i,Y_i is defined as the initialization of random variable. After, the distribution is correspondingly removing the noise. Thus it is given in equation (5)

$$J_{GL}(X,Y)=\sum_{i=1}^{l}\beta_i^{\alpha}(1-C_{\alpha,\beta_i}(X_i,Y_i)) \tag{5}$$

Here, J_{GL} is defined as generalized loss; X,Y is defined as random variable; C is denotes join distribution; α is represented the shape parameter; β is represented by the kernel bandwidth and X_i,Y_i is defined as the initialization of random variable. Finally, the noise is removed from the collected real time collected images. Then the pre-processed images are fed to Feature extractionphase.

C. Feature extraction using Synchro spline-kernelled chirplet extracting transform

In this section, SSCET [27] is proposed. Then the SSCET is extract the feature such as Geometric features likes area, slope, centroids and perimeter. The frequency-rotating, frequency-shifting operators of SCT were enhanced by the modified Synchro extracting operator upon which the SSCET technique is based; $g_\sigma(t)$ is Gaussian window is given in equation (6)

$$g_\sigma(t)=\frac{1}{\sqrt{2\pi\sigma}}.e^{-\frac{1}{2}\left(\frac{1}{\sigma}\right)^2} \tag{6}$$

Here, $g_\sigma(t)$ is denotes Gaussian window; π is denotes the constant value of the function; σ is denotes the resolution parameter of the window function and e is denotes the element of the function. The function is expressed to the phase shift of SSCET. Thus given in equation (7)

$$SCT_e=\int_{-\infty}^{\infty}g_\sigma(\tau-t_0).s(\tau).\Phi^R(\tau).\Phi^S(\tau).e^{-i\omega(\tau-t)}d\tau \tag{7}$$

Here, SCT_e is defined as phase shift of SSCET; Φ^R *and* Φ^S represents spline frequency- rotting and spline frequency- shifting operation; $g_\sigma(t)$ is denotes Gaussian window; e is denotes the element of the function; t_0 is denotes the starting stage of time; τ is denotes the length of the time and ω is denotes coefficient of the frequency. Two- dimensional of co- efficient satisfying condition is leading to discontinuous, fluctuating of time-varying features attained. Thus it is given in equation (8)

$$\omega_0=-i.\frac{\partial_t SCT_e(t,\omega)}{SCT_e(t,\omega)} \tag{8}$$

Here, ω_0 is denotes coefficient of the initial frequency; SCT_e is defined as phase shift of SSCET; ω denotes coefficient of frequency; t is denotes the time period of the frequency and ∂_t model in time–frequency analysis. Then replaced the modified Synchro extracting operator is given in equation (9)

$$\delta(\omega-\omega_0)=\begin{cases}1, & \omega=\omega_0\\ 0, & \omega\neq\omega_0\end{cases} \tag{9}$$

Here, $\delta(\omega-\omega_0)$ is denotes the real application of the coefficient; ω_0 is denotes coefficient of the initial frequency and ω is denotes coefficient of the frequency. The energy concentration in noisy environments while successfully displaying the variations of attributes that change over time. Thus it is given in equation (10)

$$SSCET(t,\omega) = SCT_e.\delta(\omega-\omega_0) \tag{10}$$

Here, $SSCET(t,\omega)$ is denotes time and coefficient of SSCET; SCT_e defines phase shift of SSCET and $\delta(\omega-\omega_0)$ denotes real application of the coefficient. Area is scaled in square units, such as cm³, m². The area of shape is 2D quantity. "Area" refers to area inside boundary or limit of closed shape. The geometry of such shape is made up of at least three sides that join to form a boundary. Thus it is given in equation (11)

$$A = L*W \tag{11}$$

Here, A is defined as Area of the two- dimensional; L is defined as the length and W is denotes the width. The ratio of y increases as x increases by certain amount known as line's slope. The slope of a line indicates its slope, or how much y grows as x increases. Everywhere along line, slope is constant, or same. Thus it is given in equation (12)

$$m = \frac{\Delta y}{\Delta x} \tag{12}$$

Here, m is represents the slope; Δy represents change in y- coordinate (vertical change); Δx represents change in x- coordinate (horizontal change).The centroid is the object's center point. The centroid of triangle is location where three triangle medians converge. It can mean location where three medians converge. A line connecting side's midpoint, triangle's opposite vertex is named median. Thus it is given in equation (13)

$$G_x = \frac{x_1 + x_2 + x_3}{3} \tag{13}$$

Here, G_x is denotes the averaging the x coordinates; x_1 , x_2 *and* x_3 are represented by vertices of the triangle. Entire length of shape's boundary known as shape's perimeter in geometry. A shape's perimeter is computed adding lengths of all of its sides, edges. It is expressed in linear units of measurement, such as feet, inches, meters, or centimetres. Thus it is given in equation (14)

$$P = 2*(L+W) \tag{14}$$

Here, P is defined as perimeter; L is defined as Length and W is defined as Width. Finally, the features are extracted by using Synchro spline-kernelled chirplet extracting Transform and Thermo dynamics-informed neural network (TINN) is used for the heritage picture collection and instructs the visual feature set. Then, the features extraction output is fed to Thermodynamics-informed neural network.

D. Heritage Picture Collection using Thermodynamics-informed neural network

In this section, Heritage Picture Collection using Thermodynamics-informed neural network (TINN) [28] is discussed. Ithas demonstrated that because of the thermo physical characteristics that supercritical fluids display close, they have the ability to produce micro confined turbulence when subjected to high-pressure. This led to increased interest in understanding when operating near pseudo-boiling transitioning area. Though, because conducting experiments at high pressure levels presents some difficulties. To make use of both the physical understanding of the state that characterizes thermo physical qualities and the supervised data of those properties. Thus it is given in equation (15)

$$L(x,S;\theta,\lambda) = \lambda_D L^D(x;\theta) + \lambda_P L^P(x,S;\theta) \tag{15}$$

Here, L represents hybrid thermodynamics- information loss function; λ_D , λ_P is represented by fixed weights otherwise penalty coefficients; S is represented by set of parameters prescribed by problem setup; θ is represented by collects weights, biases across network and λ is represented by (λ_D,λ_P) is weight vector with λ_D, λ_P loss weights corresponding to data-driven, physics-depend loss functions. By using a loss function informed by thermodynamics and composed of the residual of the state, the thermo physical limitations and ensures their fulfilment in the network design. Thus it is given in equation (16)

$$g_T(y) = \frac{T_{hw} - T_{cw}}{y_{hw} - y_{cw}}(y - y_{cw}), \qquad y \in \Omega_y \tag{16}$$

Here, $g_T(y)$ is represented by extended linear formulation; y is represented by coordinate of the domain; T_{hw} and y_{hw} is represented by projection transformation and T_{cw}, y_{cw} is represented by heritage. By altering the network architecture, particularly the network is presented. Thus it is given in equation (17)

$$\hat{z}(x,S;\theta) = (1-l(y))\, g(y) + l(y)\, L^L(x,S;\theta), \qquad x \in \Omega \tag{17}$$

Here, $\hat{z}$ represents $\hat{z} = (\hat{p},\hat{T})$ is prediction vector; g is represented by vector of extended pixel boundary conditions; $L^L(x,S;\theta)$ represents network output; Ω represented by vector domain, l is represented by length of function. Thus it is given in equation (18)

$$\begin{cases} l(y) = 0, & y \in \delta\Omega_y \\ l(y) > 0, & y \in \Omega_y - \delta\Omega_y \end{cases} \tag{18}$$

Here, y is represented by coordinate of the domain; l is represented by the satisfying function and Ω is represented by input features vector domain. The image process allows to analytically choosing the l function. Thus it is given in equation (19)

$$l(y) = \left[\frac{4}{L_y^2}(y - y_{cw})(y_{hw} - y) \right]^2, \qquad y \in \Omega_y \tag{19}$$

Here, l is represented by the satisfying function; y is represented by coordinate of the domain; Ω is represented by input features vector domain; y_{cw} is represented by cold wall; y_{hw} is represented by hot wall and L is represented by total length of the domain. Finally, TINNaccurately captures theheritage picture collection. Due to its convenience, pertinence, AI-depend optimization approach is taken into account in TINN network. Here, BAOA is employed to optimize the TINN, for tuning weight, bias parameter of TINN.

E. Optimization using Binary Arithmetic Optimization Algorithm

The proposed BAOA is utilized to enhance weights parameters $(\hat{p},\hat{T})$ of proposed TINN [29]. Recently, a metaheuristic algorithm called BAOA was presented. It has demonstrated strong performance in multiple benchmark tests. It is a metaheuristic makes advantage of distribution behaviour of the primary arithmetic operators, including addition, subtraction, division, and multiplication. The Binary Arithmetic Optimization Algorithm (BAOA) in binary form, which addresses the feature selection issue in classification.

1) Stepwise process for BAOA

Here, stepwise process for obtaining appropriate TINN values using BAOA is described here. To creates a uniformly distributed population for optimizing the ideal TINN parameters. The entire step method is then presented in below

Step 1:Initialization phase

Initial population of BAOA is, initially generated by randomness. Then the initialization is derived in equation (20)

$$z = \begin{bmatrix} z_{1,1} & z_{1,2} \ldots . z_{1,N} \\ z_{2,1} & z_{2,2} \ldots . z_{1,N} \\ \ldots\ldots & \ldots\ldots \quad \ldots\ldots \\ z_{N,1} & z_{N,2} \ldots z_{N,D} \end{bmatrix} \tag{20}$$

Where, z denotes the total population of binary arithmetic; N denotes the n^{thh} number of BAOA and D represents the distance between the prey and BAOA.

Step 2:Random generation phase

Input weight parameter $\hat{p},\hat{T}$ developed randomness via BAOA method.

Step 3:Fitness function

Generate random solution from values of initialization. It is evaluated depend on equation given in (21),

$$Fitness\ function = Optimizing[(\hat{p},\hat{T})] \tag{21}$$

Step 4: Exploration phase $(\hat{p},\hat{T})$

Exploring potential areas for improvement and learning about the characteristics of the target binary arithmetic operations comprise the exploration phase of a binary arithmetic optimization process. The exploration stage lays the groundwork for the next stages of optimization, when certain tactics can be put into practice and evaluated in light of the discoveries discovered. It is crucial for improving the optimization strategy. For applications like binary classification, where predict the likelihood of an event happening or not happening, the sigmoid function comes in handy. Thus it is given in equation (22)

$$sigmoid(x) = \frac{1}{1+e^{-10(x-0.5)}} \tag{22}$$

Here, $sigmoid(x)$ is represented by original exploration stage; $e^{-10(x-0.5)}$ is represented by binary exploration phase. Likewise, position updating of exploration phase can be evaluated. Thus it is given in equation (23)

$$B_2\left(x_{i,j}(t+1)\right) = \begin{cases} 1 & if\ sigmoid\left(x_{i,j}(t+1)\right) \geq rand \\ 0 & otherwise \end{cases} \tag{23}$$

Where, $x_{i,j}(t+1)$ represents original exploration stage; $B_2\left(x_{i,j}(t+1)\right)$ represented by modified binary position of exploration phase in iteration t and $rand$ represented by number created at random from distributions uniform. The flow chart of BAOA is given in Figure. 2

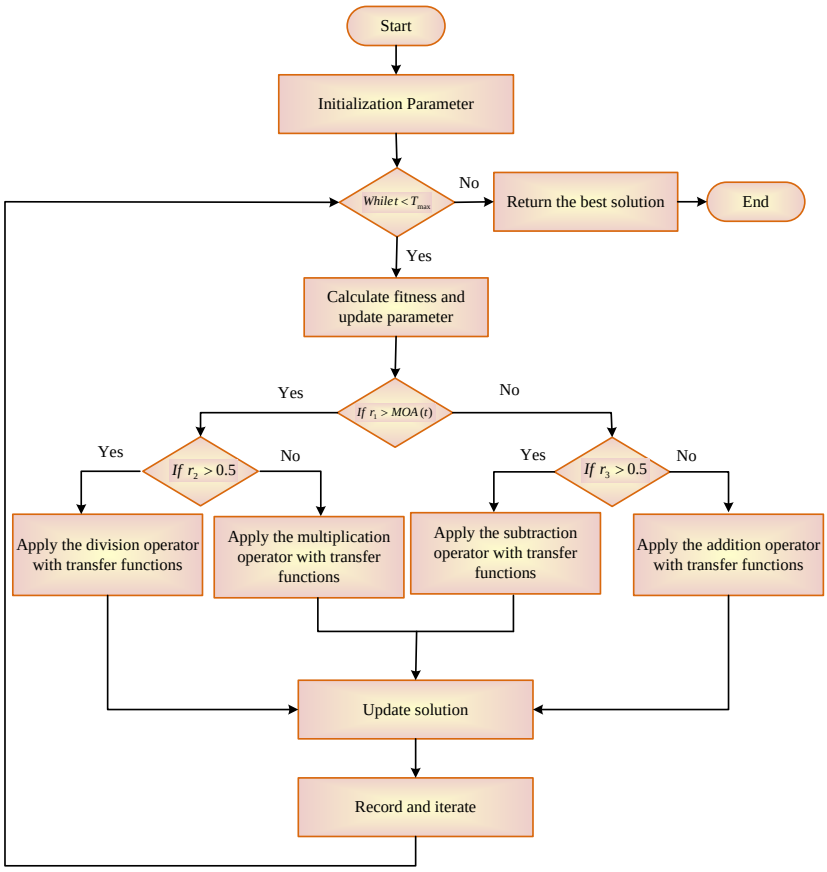

Figure2: Flowchart of BAOA optimizing for TINN

Step 5:Exploitation phase

In order to improve the performance of targeted binary arithmetic operations, particular solutions found during the exploration phase are put into practice during the exploitation phase of binary arithmetic optimization. The objective of the exploitation phase is to put the optimization strategies into practice and validate them in order to make sure that the performance gains are substantial and meet the needs of the

intended application. Based on feedback and real-world usage, it could be required to continuously monitor and refine. Then the fitness function is utilized to improve the phase. Thus it is given in equation (24)

$$fitness = \alpha\rho_R(Y) + \beta\frac{|K|}{|N|} \tag{24}$$

Here, $\alpha\rho_R(Y)$ is denotes the parameter of the given function; α is denotes the parameter of $[0,1]$; β is denotes the parameter of $(1-\alpha)$; $|K|$ is denotes the number, $|N|$ denotes original number of dataset. Metric accurate is a set of characteristics. Thus it is given in equation (25)

$$MCA = \frac{1}{N}\sum_{k=1}^{N} AvgAcc^k \tag{25}$$

Here, MCA is denotes mean of heritage accuracy; N denotes the total number of accuracy and $AvgAcc^k$ is denotes the average gain in accuracy at k run.

Step6: Termination

The weight parameter value of generator $(\hat{p},\hat{T})$ from Thermodynamics-informed neural network is optimized by utilizing BAOA; and it will repeat step 3 until it obtains its halting criteria $z = z+1$. The BVR-SE-IMIH-TINN effectively assesses the quality of Virtual Reality-Based Spatial Experience and Interaction Model of Industrial Heritage higher accuracy, lessening computational time and error.

IV. RESULT WITH DISCUSSION

Experimental results of BVR-SE-IMIH-TINNare discussed in this section. The proposed BVR-SE-IMIH-TINN method is implemented in Java Applet-depend method to realize virtual roaming of viewing panoramic images. Obtained outcome of the proposed BVR-SE-IMIH-TINNapproach is analyzed with existing, such as ISM-VLHP-AML, DPH-CH-VRT and RI-HCE-VAR systems.

A. Performance Measures

Performance of proposed method is examined utilizing accuracy, recall, Precision, FI-Score, specificity and computational time.

1) Accuracy

Accuracy describes detection rate that are correctly classified. The formula is derived in equation (26).

$$Accuracy = \frac{TP+TN}{FN+TP+FP+TN} \tag{26}$$

Here, TP denotes true positive, TN signifies true negative, FN denotes false negatives and FP signifies false positive.

2) Recall

Recall is a performance metric commonly used in binary tasks. It is given in equation (27)

$$\mathrm{Re}call = \frac{TP}{FN+TP} \tag{27}$$

3) Precision

It estimates positive result count while diagnosis of leaf diseases. Then the formula is derived in equation (28).

$$\mathrm{Pr}ecision = \frac{TP}{FP+TP} \tag{28}$$

4) F1- Score

The performance equation is provided in and the evaluation parameter of F1-score is analyzed. Thus given in equation (29)

$$F1-Score = 2\times\frac{\mathrm{Pr}ecision\times\mathrm{Re}call}{\mathrm{Pr}ecision+\mathrm{Re}call} \tag{29}$$

5) Specificity

It estimates the proportion of negative instances and expressed in equation (30)

$$Specificity = \frac{TN}{TN+FP} \tag{30}$$

6) Computation Time

The computation time is very depending on the specific context, type of computation and the algorithm or method involved. Thus, given in equation (31)

$$T(n) = a\, f(n) + b \tag{31}$$

Here, $T(n)$ is represented by computational time; n is represents the input size; a is represents the constant factor; $f(n)$ is represents the time complexity function describing the input size; b is represents the constant of additional fixed overhead.

B. Performance Analysis

Figure 3 to 8 shows simulation results of BVR-SE-IMIH-TINN technique. The BVR-SE-IMIH-TINN is analysed to the existing ISM-VLHP-AML, DPH-CH-VRT and RI-HCE-VAR respectively.

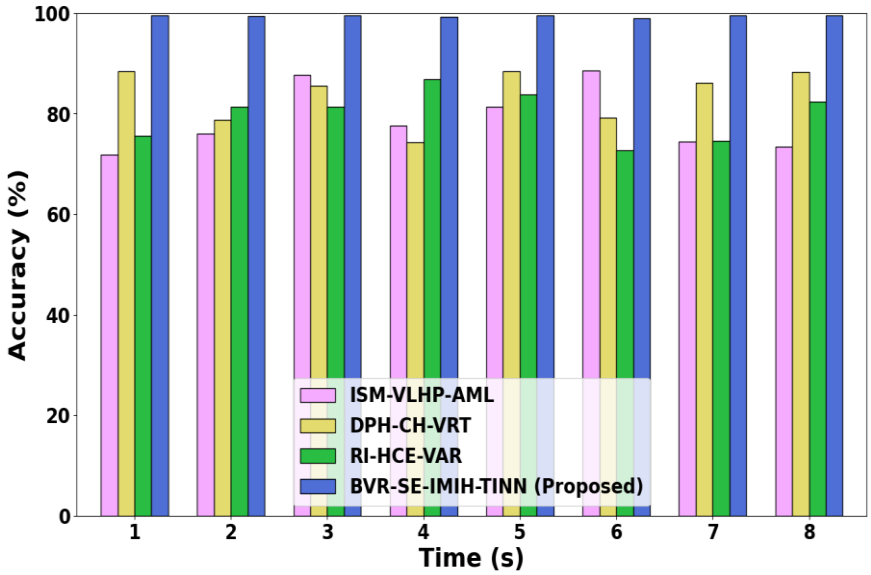

Figure3: Accuracy analysis

Figure 3 depicts accuracy analysis. The BVR-SE-IMIH-TINN attains 18.41%, 24.08% and 32.57% greater accuracy at number of time taken at 2; 17.64%, 23.21% and 32.91% greater accuracy at number of time taken at 4; 17.12%, 23.41% and 32.90% greater accuracy at number of time taken at 6; 20.85%, 22.96% and 23.23% greater accuracy at number of time taken at 8;which is analyzed with ISM-VLHP-AML, DPH-CH-VRT and RI-HCE-VAR methods respectively.

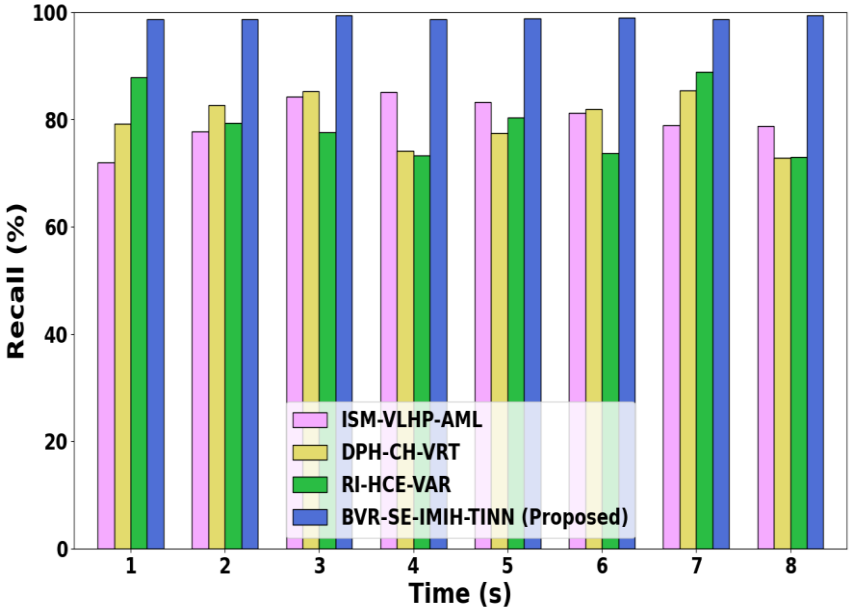

Figure4: Recall analysis

Figure 4 depicts recall analysis. The BVR-SE-IMIH-TINN attains 19.21%, 20.08% and 21.57% higher recall at number of time taken at 2; 18.64%, 21.21% and 30.91% higher recall at number of time taken at 4; 22.12%, 23.41% and 31.90% higher recall at number of time taken at 6;25.23%, 26.33% and 27.90% higher

recall at number of time taken at 8;which is analyzed with ISM-VLHP-AML, DPH-CH-VRT and RI-HCE-VAR methods respectively.

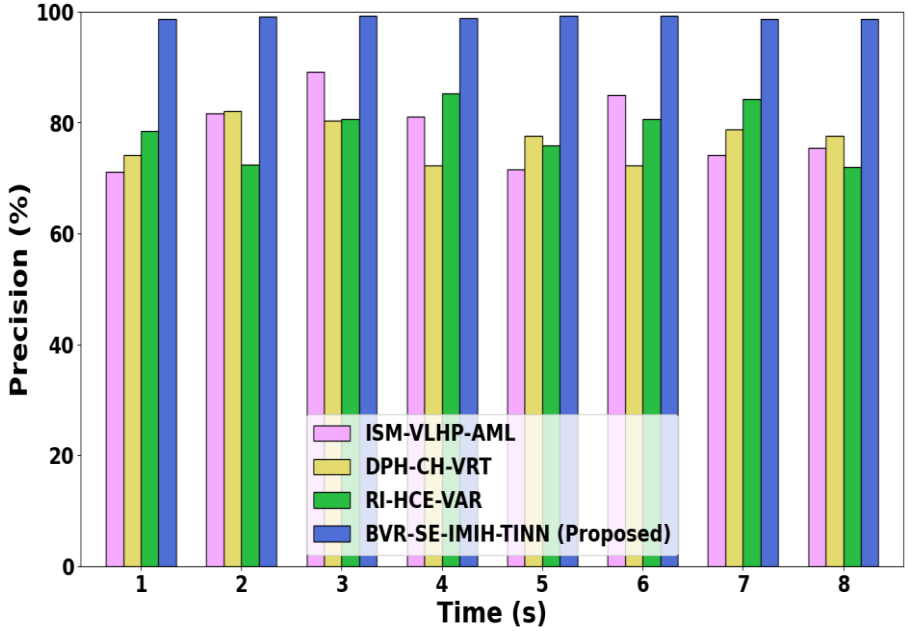

Figure5: Precision analysis

Figure 5 depicts precision analysis. The BVR-SE-IMIH-TINN attains 20.31%, 21.08% and 22.57% higher Precision at number of time taken at 2; 18.64%, 21.21% and 30.91% higher Precision at number of time taken at 4; 27.12%, 29.41% and 31.10% higher Precision at number of time taken at 6; 25.55%, 26.98% and 27.10% higher Precision at number of time taken at 8;which is analyzed with ISM-VLHP-AML, DPH-CH-VRT and RI-HCE-VAR methods respectively.

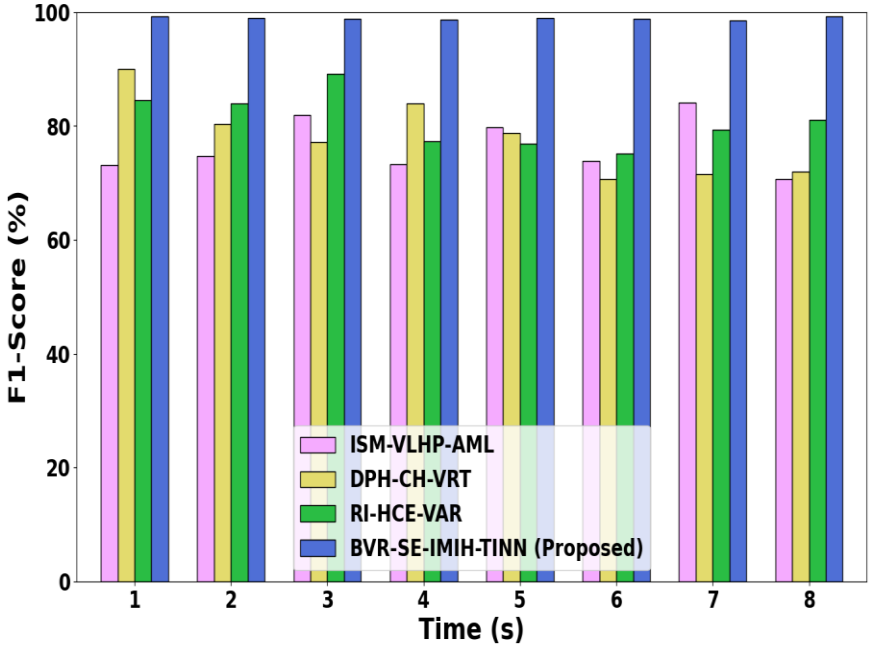

Figure6: F1-score analysis

Figure 6 depicts F1-score analysis. The BVR-SE-IMIH-TINN attains 22.20%, 23.10% and 25.57% higherF1- Score at number of time taken at 2; 26.64%, 28.21% and 30.10% higher F1- Score at number of time taken at 4; 29.12%, 29.41% and 31.10% higher F1- Score at number of time taken at 6;27.20%, 28.30% and 29.60% higher F1- Score at number of time taken at 8; which is analyzed with ISM-VLHP-AML, DPH-CH-VRT and RI-HCE-VAR methods respectively.

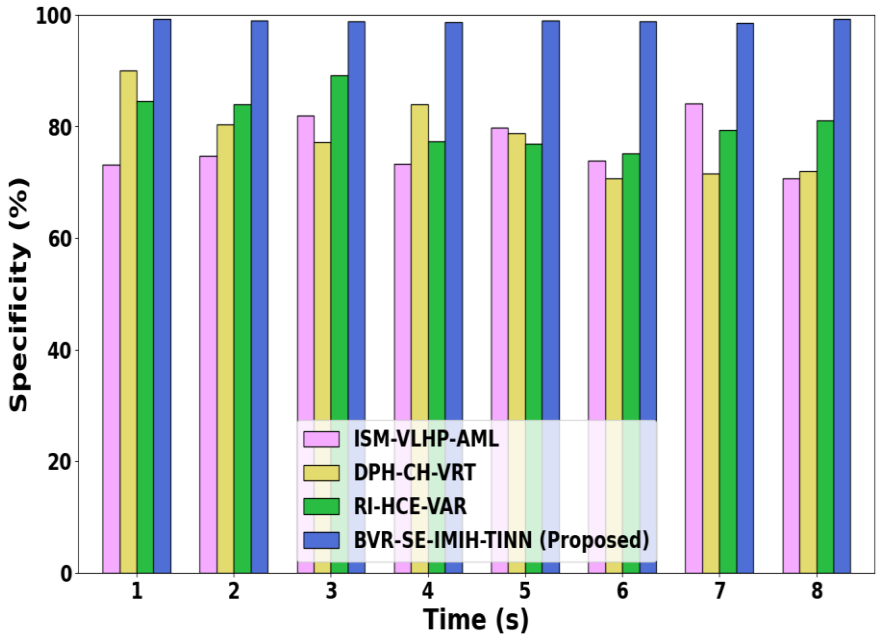

Figure7: Specificity analysis

Figure 7 depicts specificity analysis. The BVR-SE-IMIH-TINN attains 25.20%, 26.40% and 28.57% higher Specificity at number of time taken at 2; 28.64%, 29.21% and 32.10% higher Specificity at number of time taken at 4; 28.12%, 29.41% and 30.10% higher Specificity at number of time taken at 6; 21.25%, 23.60% and 25.30% higher Specificity at number of time taken at 8; which is analyzed with ISM-VLHP-AML, DPH-CH-VRT and RI-HCE-VAR methods respectively.

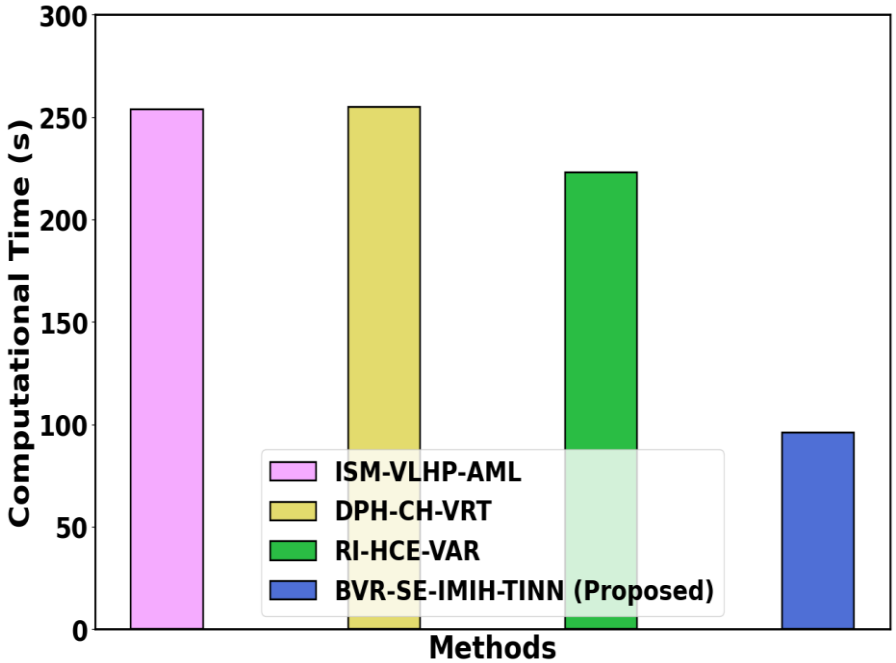

Figure 8: Computation time analyses

Figure 8 shows performance of computation time analysis. The BVR-SE-IMIH-TINN technique attains 22.5%, 24.9%, and 26.3% lesser computation time analysed with existing techniques likes ISM-VLHP-AML, DPH-CH-VRT and RI-HCE-VAR methods respectively.

C. Discussion

An efficient proposed BVR-SE-IMIH-TINN are proposed for Virtual Reality-Based Spatial Experience and Interaction Model of Industrial Heritage; the regression functions the pre- processing using GMMCKF. Followed by, Feature Extraction using SSCET; then, extracted image is using TINN. The next Interaction Model of Industrial Heritage TINN and Optimization of TINN using BAOA; As a result, an Industrial Heritage is eliminated The specificity values of BVR-SE-IMIH-TINN are 25.20%, 26.40%, 28.57% higher than existing

techniques likes ISM-VLHP-AML, DPH-CH-VRT and RI-HCE-VAR methods respectively. Similar to this, the Virtual Reality-Based Spatial Experience and Interaction Model of Industrial Heritage is proposed 97.92% analyzed with Interaction Model of Industrial Heritage is 80.42%. The proposed method BVR-SE-IMIH-TINN has high accuracy and F1- Score evaluation metrics than existing methods. Therefore, the comparative methods are expensive than the proposed technique. As a result, the proposed approach Virtual Reality-Based Spatial Experience and Interaction Model's Industrial Heritage is more effectively and efficiently.

V. CONCLUSION

In this section, Construction of Spatial Experience and Interaction Model of Industrial Heritage Based on Virtual Reality Technology (BVR-SE-IMIH-TINN) are successfully executed. Proposed BVR-SE-IMIH-TINN method is applied in Java Applet-depend method to realize virtual roaming of viewing panoramic images. Then the images are extracted from image process of virtual reality, for classifying the virtual Detection. According to the experimental results, BVR-SE-IMIH-TINN performed better when used with the Co-training technique than when used separately regards FI-Score, precision and specificity. The performance of BVR-SE-IMIH-TINN approach attains 18.64%, 21.21% and 30.91% higher Precision, 28.12%, 29.41% and 30.10% higher Specificity and 22.20%, 23.10% and 25.57% higher F1- Score and 26.3% lower Computational Time when analyzed with existing methods like ISM-VLHP-AML, DPH-CH-VRT and RI-HCE-VAR respectively.

REFERENCE

[1] Zhao, L. (2023). Personalized healthcare museum exhibition system design based on VR and deep learning driven multimedia and multimodal sensing. *Personal and Ubiquitous Computing*, *27*(3), 973-988.

[2] Zhang, Q. (2022). Development and analysis of educational virtual reality system using static image. *Mobile Information Systems*, *2022*, 1-9.

[3] Sperlí, G. (2021). A cultural heritage framework using a deep learning based chatbot for supporting tourist journey. *Expert Systems with Applications*, *183*, 115277.

[4] Song, F. (2021). 3D virtual reality implementation of tourist attractions based on the deep belief neural network. *Computational Intelligence and Neuroscience*, *2021*.

[5] Zhong, H., Wang, L. & Zhang, H. (2021). The application of virtual reality technology in the digital preservation of cultural heritage. *Computer Science and Information Systems*, *18*(2), 535-551.

[6] Lampropoulos, G., Keramopoulos, E. & Diamantaras, K. (2020). Enhancing the functionality of augmented reality using deep learning, semantic web and knowledge graphs: A review. *Visual Informatics*, *4*(1), 32-42.

[7] Wang, L., Tang, D., Liu, C., Nie, Q., Wang, Z. & Zhang, L. (2022). An Augmented Reality-Assisted Prognostics and Health Management System Based on Deep Learning for IoT-Enabled Manufacturing. *Sensors*, *22*(17), 6472.

[8] Li, X., Shan, Y., Chen, W., Wu, Y., Hansen, P. & Perrault, S. (2021). Predicting user visual attention in virtual reality with a deep learning model. *Virtual Reality*, 1-14.

[9] Deshpande, S., Padalkar, S. & Anand, S. (2023). IIoT based framework for data communication and prediction using augmented reality for legacy machine artifacts. *Manufacturing Letters*, *35*, 1043-1051.

[10] Li, H. (2022). 3D indoor scene reconstruction and layout based on virtual reality technology and few-shot learning. *Computational Intelligence and Neuroscience*, *2022*.

[11] Estrada, J., Paheding, S., Yang, X. & Niyaz, Q. (2022). Deep-learning-incorporated augmented reality application for engineering lab training. *Applied Sciences*, *12*(10), 5159.

[12] Khan, F.A. & Ibrahim, A.A. (2023). Non-Fungible Token based Smart Manufacturing to scale Industry 4.0 by using Augmented Reality, Deep Learning and Industrial Internet of Things. *International Journal on Perceptive and Cognitive Computing*, *9*(2), 62-72.

[13] Huy, D.T.N., Hang, N.T., Thang, T.D., Thuy, P.T. and Thuy, V.X. (2021). Virtual Reality Technology and Simulation Technology to Development of Smart Travelling in the Time of Industrial Revolution 4.0. *Technology*.

[14] Rai, R., Tiwari, M.K., Ivanov, D. & Dolgui, A. (2021). Machine learning in manufacturing and industry 4.0 applications. *International Journal of Production Research*, *59*(16), 4773-4778.

[15] Checa, D., Urbikain, G., Beranoagirre, A., Bustillo, A. & Lopez de Lacalle, L.N. (2022). Using Machine-Learning techniques and Virtual Reality to design cutting tools for energy optimization in milling operations. *International Journal of Computer Integrated Manufacturing*, *35*(9), 951-971.

[16] Seeliger, A., Weibel, R.P. & Feuerriegel, S. (2022). Context-Adaptive Visual Cues for Safe Navigation in Augmented Reality Using Machine Learning. *International Journal of Human–Computer Interaction*, 1-21.

[17] Sindu, I.G.P., Hartati, R.S., Sudarma, M. & Gunantara, N. (2023). Systematic Literature Review of Machine Learning in Virtual Reality and Augmented Reality. *JurnalNasionalPendidikanTeknikInformatika: JANAPATI*, *12*(1).

[18] Moba, C. (2023). A Legal Virtual Reality Narrative Reconstruction of Intangible Cultural Heritage-Boat Shaped House in Hainan, China. *J. Legal Ethical &Regul. Isses*, *26*, 1.

[19] Tiwari, R., Duhan, N., Mittal, M., Anand, A. & Khan, M.A. eds., (2022). *Multimedia Computing Systems and Virtual Reality*.CRC Press.

[20] Fu, Y., Guo, T. & Zhao, X. (2021). Intelligent splicing method of virtual reality lingnan cultural heritage panorama based on automatic machine learning. *Mobile Information Systems*, *2021*, 1-10.

[21] Zhang, W. (2022). Key Technologies of Digital Protection of Historical and Cultural Heritage Based on Virtual Reality Technology. *Mobile Information Systems*, *2022*.

[22] Paulauskas, L., Paulauskas, A., Blažauskas, T., Damaševičius, R. & Maskeliūnas, R. (2023). Reconstruction of Industrial and Historical Heritage for Cultural Enrichment Using Virtual and Augmented Reality. *Technologies*, *11*(2), 36.

[23] Deng, X., Kim, I.T. & Shen, C. (2021). Research on convolutional neural network-based virtual reality platform framework for the intangible cultural heritage conservation of China hainan Li nationality: boat-shaped house as an example. *Mathematical Problems in Engineering*, *2021*, 1-16.

[24] Khan, M.A., Israr, S., S Almogren, A., Din, I.U., Almogren, A. & Rodrigues, J.J. (2021). Using augmented reality and deep learning to enhance Taxila Museum experience. *Journal of Real-Time Image Processing*, *18*, 321-332.

[25] Rinaldi, A.M., Russo, C. & Tommasino, C. (2022). An Augmented Reality CBIR System Based on Multimedia Knowledge Graph and Deep Learning Techniques in Cultural Heritage. *Computers*, *11*(12), 172.

[26] Li, S., Shi, D., Lou, Y., Zou, W. & Shi, L. (2023). Generalized Multi-kernel Maximum Correntropy Kalman Filter for Disturbance Estimation. *IEEE Transactions on Automatic Control*.

[27] Ma, Y., Lv, Y., Yuan, R. & Ge, M. (2021). Synchro spline-kernelled chirplet extracting transform: A useful tool for characterizing time-varying features under noisy environments and applications to bearing fault diagnosis. *Measurement*, *181*, 109574.

[28] Masclans, N., Vázquez-Novoa, F., Bernades, M., Badia, R.M. & Jofre, L. (2023). Thermodynamics-informed neural network for recovering supercritical fluid thermophysical information from turbulent velocity data. *International Journal of Thermofluids*, *20*, 100448.

[29] Bansal, P., Gehlot, K., Singhal, A. & Gupta, A.(2022). Automatic detection of osteosarcoma based on integrated features and feature selection using binary arithmetic optimization algorithm. *Multimedia Tools and Applications*, *81*(6), 8807-8834.